

Formation control of double integrators over directed graphs using bearings and bearing rates

Susmitha T Rayabagi, Debasattam Pal, and Dwaipayan Mukherjee

Abstract— Bearing-only formation control problem for agents over directed graphs, due to the loss of symmetry in the sensing graph, has been explored sparingly in comparison to the undirected counterpart. The few existing results mainly consider single integrator agents that achieve stationary formations. This paper studies the problem of bearing-only formation control for double integrator agents under a leader-first follower (LFF) structure where the underlying graph is directed acyclic in nature. We characterize the equilibrium points under our proposed control law and present local stability analysis around them. We further show that scale of the formation can be controlled purely through bearings by considering the leader’s physical dimensions to be non-trivial.

I. INTRODUCTION

Technological advancement in recent years has paved the way for synthesizing distributed engineering systems such as multi-vehicle systems, sensor networks [1], which have wide range of applications in automated highways, satellite formations, search and rescue operations [2]. Decentralized control of such multi-agent systems has attractive advantages such as low operational costs, high robustness, strong adaptability. When dealing with multiple mobile agents, formation control is of significance and finds applications in underwater exploration, target detection, surveillance using unmanned aerial vehicles, etc.

The main goal of formation control is to maintain a desired formation shape while performing tasks demanded by the mission. In order to do so, the agents are required to satisfy a set of constraints with respect to their neighboring agents. Depending on the type of constraints imposed, formation control can be classified as displacement-based, distance-based, and bearing-based formation control [3]. Distance rigidity theory emerged as a consequence of detailed investigations on distance-based and displacement-based formation control strategies [2], [4]–[6]. Distance-based and displacement-based control laws require relative position information or range information, which entails relying on external positioning systems such as GPS. However GPS cannot be used in environments like deep space. Use of onboard sensors presents a practical solution to such problems. Cameras are popularly used as onboard sensors [7], which provide more reliable relative bearing measurements with respect to a target than the corresponding range information [8]. These cameras can also provide relative bearing rates

using optical flow based on the pin-hole camera model [9], due to which the study of bearing based and bearing-only formation control has been of particular interest. Bearing based and bearing-only control laws for multi-agent systems over undirected graphs have been studied extensively [9]–[11]. Undirected graphs imply bidirectional sensing of bearings, whereas directed graphs entail one way sensing, which reduces sensing burden on the agents. The control laws for the undirected case are mostly some form of gradient or modified gradient based laws due to the symmetry in the sensing graph. This simplifies the stability analysis considerably, compared to the directed case, since the choice of a Lyapunov candidate/function is often apparent. However, with a directed sensing graph, the symmetry is lost and therefore similar techniques of analysis cannot be employed. Several studies on bearing-based and bearing-only formation control under directed sensing topologies for single integrators have been carried out in recent years [12]–[14]. However, double integrators are realistic since they capture the dynamics of omni-directional ground vehicles and unmanned air vehicles. Another crucial aspect is that these results are applicable to stationary target formations rather than to formation tracking. In [15] the authors studied LFF formation control problem with double integrators for time varying formations. However, the agents were capable of measuring relative velocities. Furthermore, the desired relative positions were used to decide the formation scale. To the best of our knowledge, there has been no work that studies the formation control problem over directed topologies for double integrators that rely only on relative bearing and relative bearing rates. Motivated by this, we studied such a control law for agents in two dimensional euclidean space in [16] and presented some preliminary results. However, the equilibrium set was not characterized and no stability analysis had been carried out as the Jacobian evaluated at the claimed desired equilibrium was singular. No guarantee on the formation scale could be provided either. In our current work, we consider that the leader has a circular disk shape of finite constant radius. This allows us to control the scale of the formation without requiring any distance measurements. This consideration is not restrictive as any vehicle moving in a two-dimensional plane has a non-trivial dimension, as in [17]–[19]. We then prove the existence of two equilibria for our proposed control law and provide local stability analysis for each of the equilibria. Finally, we provide simulations to compare our proposed control strategy with the one proposed in [16].

*This work was supported in part by an ISRO (Indian Space Research Organization) funded project bearing code RD/0120-ISROC00-007.

The authors (srayabagi@iitb.ac.in), (debasattam@ee.iitb.ac.in), (dm@ee.iitb.ac.in) are with the Department of Electrical Engineering, Indian Institute of Technology Bombay, Powai, Mumbai- 400076, India

II. PRELIMINARIES AND PROBLEM FORMULATION

A. Notation

Consider a multi-agent system of n agents with one agent being the leader (labelled as agent 1) and the remaining $n-1$ being followers. Let $\mathcal{G}(\mathcal{V}, \mathcal{E})$ or \mathcal{G} be a directed graph with vertex or node set $\mathcal{V} = \{v_1, \dots, v_n\}$ and $|\mathcal{V}| = n$. The edge set, \mathcal{E} , consists of $|\mathcal{E}| = m$ ordered pairs of vertices from the vertex set, defined as $\mathcal{E} = \{(v_i, v_j) | v_i, v_j \in \mathcal{V}, v_i \neq v_j\} \subseteq \mathcal{V} \times \mathcal{V}$. The vertex v_j is said to be a neighbor of vertex v_i if $(v_i, v_j) \in \mathcal{E}$, and the set of all neighbors for vertex v_i is denoted as $\mathcal{N}_i = \{v_j \in \mathcal{V} | (v_i, v_j) \in \mathcal{E}\}$. Consider a set of n points in the two-dimensional Euclidean space, $p_i \in \mathbb{R}^2$, $i \in \{1, 2, \dots, n\}$ that are uniquely mapped to each vertex $v_i \in \mathcal{V}$. The stacked vector $p = [p_1^T, \dots, p_n^T]^T \in \mathbb{R}^{2n}$ is called the configuration of \mathcal{G} . The configuration, p , along with the directed graph, \mathcal{G} , define a framework in \mathbb{R}^2 , denoted by $\mathcal{G}(p)$. Given a framework, $\mathcal{G}(p)$, we define the following

$$e_k = e_{ij} := p_j - p_i; \quad g_k = g_{ij} := \frac{e_k}{\|e_k\|} \quad \forall k \in \{1, \dots, m\}$$

as the edge vector and bearing vector for the k^{th} directed edge $(v_i, v_j) \in \mathcal{E}$, respectively. Note the slight abuse of notation in the subscript of the edge vector and the bearing vector, where a single subscript indicates the edge index, while a double subscript indicates the vertices on which the edge is incident. Depending on the context and the use, we will employ either notation for the edge vector. The unit vector, g_{ij} , is the relative bearing of p_j to p_i . We denote distance between the points p_i and p_j with $d_{ij} = \|p_j - p_i\| = \|e_{ij}\|$. Here $\|\cdot\|$ is the L_2 vector norm or the induced L_2 norm of a matrix. The matrices $\mathbf{0}_k, I_k$ denote the zero and identity matrices of size $k \times k$, respectively.

For a given unit vector, $x \in \mathbb{R}^2$, the orthogonal projection matrix is defined as $P_x = I_2 - xx^T$. The matrix P_x is symmetric, i.e., $P_x = P_x^T$, and idempotent, i.e., $P_x^2 = P_x$. Further, we have $P_x x = 0$, indicating that $\text{Null}(P_x) = \text{span}\{x\}$, and P_x has eigenvalues $\{0, 1\}$. From the definition of g_{ij} , the bearing rate or the time derivative of g_{ij} can be obtained as $\dot{g}_{ij} = \frac{P_x g_{ij}}{\|e_{ij}\|} \dot{e}_{ij} = \frac{P_x g_{ij}}{\|e_{ij}\|} (\dot{p}_j - \dot{p}_i)$. It immediately follows from the expression for g_{ij} and the properties of the orthogonal projection matrix above that $g_{ij}^T \dot{g}_{ij} = e_{ij}^T \dot{g}_{ij} = 0$, implying that \dot{g}_{ij} is orthogonal to g_{ij} and e_{ij} .

B. Bearing based Henneberg construction

The bearing based Henneberg construction is employed to construct the underlying graph that has the LFF structure. A graph with n vertices can be constructed in $n-1$ steps, every step after the first effectively adds two directed edges, hence there are $2(n-2) + 1 = 2n-3$ directed edges. All the vertices except v_1 and v_2 have two neighbors. A directed edge $(v_i, v_j) \in \mathcal{E}$ assigns the task of controlling the bearing g_{ij} to vertex/agent v_i . The construction starts with a simple graph with two vertices, v_1, v_2 , and a directed edge (v_2, v_1) . Each step thereafter involves performing two operations, *vertex addition* and *edge splitting*, to build the underlying graph, as illustrated in Fig 1.

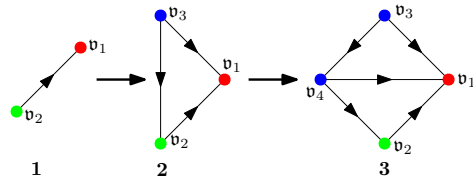


Fig. 1. An LFF graph with 4 vertices, Vertex addition is performed in step 2 and edge splitting is performed in step 3

Vertex addition: A new vertex along with two directed edges is added to the existing graph as shown in Step 2 of Fig 1. Vertex v_3 is added with two directed edges (v_3, v_2) and (v_3, v_1) , hence v_3 has two neighbors v_1 and v_2 .

Edge splitting: A vertex v_i with two neighbors is selected and an edge with one of its neighbors is removed. A new vertex v_k is added along with three directed edges. In step 3 of Fig 1, the edge (v_3, v_2) is removed, and vertex v_4 is added along with 3 directed edges (v_3, v_4) , (v_4, v_2) and (v_4, v_1) . A detailed account of bearing-based Henneberg constructions is presented in [14], [20].

C. Problem formulation

Consider a system of n agents in \mathbb{R}^2 , where each agent is modelled by a double integrator given by

$$\dot{p}_i(t) = v_i(t) \quad \dot{v}_i(t) = u_i(t), \quad (1)$$

where $p_i \in \mathbb{R}^2$, $v_i(t) \in \mathbb{R}^2$ and $u_i(t) \in \mathbb{R}^2$ are the position, velocity, and acceleration input to be designed for agent i , respectively. Each agent is capable of sensing bearing vectors and bearing rates relative to their neighbors, with respect to a common global frame of reference.

Definition 1 (Target Formation): An LFF target formation $(\mathcal{G}, p^*(t))$ satisfies the desired constant interneighbor bearings $\{g_{ij}^*\}_{(v_i, v_j) \in \mathcal{E}}$ and translates with a velocity that is equal to the constant leader velocity v_1^* .

The existence of such a translating target formation is a direct consequence of [14, Lemma 2]. In summary, the following assumptions are made for the n agent system.

Assumption 1: The underlying graph, \mathcal{G} , of the target formation is generated using the bearing based Henneberg construction and each agent can measure bearing and bearing rate vectors with respect to their neighbors.

The assignment of bearings in bearing-based Henneberg construction is such that the resulting LFF formation guarantees bearing rigidity [20].

Assumption 2: The desired position, $p_i^*(t)$, of agent v_i ($3 \leq i \leq n$) in the target formation $(\mathcal{G}, p^*(t))$ is not collinear with its 2 neighboring agents v_j and v_k , i.e., $g_{ij}^* \neq \pm g_{ik}^*$.

Assumption 3: The leader has a circular disk shape with constant radius $r \in \mathbb{R}_+$, and the first follower v_2 measures two bearing vectors relative to the leader: g_{21} , measured with respect to the center of the aforesaid disk, and \bar{g}_{21} , measured along a tangent to the disk passing through p_2 . Agent v_2 also measures the corresponding bearing rates \dot{g}_{21} and $\dot{\bar{g}}_{21}$.

Let \bar{p}_1 be the point on the disk with respect to which \bar{g}_{21} is measured. Similar to other relative bearing vectors, define

$\bar{g}_{21} = \frac{\bar{p}_1 - p_2}{\|\bar{p}_1 - p_2\|} = \frac{\bar{e}_{21}}{\|\bar{e}_{21}\|}$, with $\bar{e}_{21} = \bar{p}_1 - p_2$. From Fig 2, we have $\bar{p}_1 = p_1 + \hat{r}$, where \hat{r} is the radius vector ($\|\hat{r}\| = r$). Both p_1 and \bar{p}_1 move with same velocity, i.e, $\dot{p}_1 = \dot{\bar{p}}_1 = v_1$. Since the agent v_2 senses \bar{g}_{21} along the tangent to the disk, it tracks the outermost point along the disk using its sensor. Hence, the position \bar{p}_1 is invariant under leader's rotation.

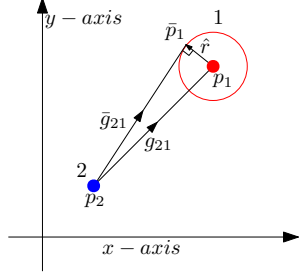


Fig. 2. Agent 2 measuring two bearings relative to the leader

Assumption 4: No inter-neighbour agent collisions occur during the formation evolution.

The bearing-only formation control problem is as follows.

Problem 1: Under the Assumptions 1 – 4, with agent dynamics given in (1), design acceleration inputs for the $n - 1$ followers using only the instantaneous bearings $\{g_{ij}\}_{(v_i, v_j) \in \mathcal{E}}$ and bearing rates $\{\dot{g}_{ij}\}_{(v_i, v_j) \in \mathcal{E}}$, such that a given target formation is achieved.

III. MAIN RESULTS

The following bearing-only formation control law is proposed for the $n - 2$ followers ($i \in \{3, \dots, n\}$)

$$\begin{aligned} \dot{p}_i &= v_i \\ \dot{v}_i &= -k_p \sum_{j \in \mathcal{N}_i} P_{g_{ij}} g_{ij}^* + k_v \sum_{j \in \mathcal{N}_i} \dot{g}_{ij} \end{aligned} \quad (2)$$

and for the first follower ($i = 2$)

$$\begin{aligned} \dot{p}_2 &= v_2 \\ \dot{v}_2 &= -k_p P_{g_{21}} g_{21}^* - k_p P_{\bar{g}_{21}} \bar{g}_{21}^* + k_v \dot{g}_{21} + k_v \dot{\bar{g}}_{21} \end{aligned} \quad (3)$$

where k_p and k_v are constant positive control gains.

1) The leader

The leader's motion is governed by $\dot{p}_1 = v_1$, $\dot{v}_1 = 0$ and moves with a constant desired velocity $v_1 = v_1^*$. Its position is given by $p_1^* = p_1(0) + v_1^* t$ for all $t \geq 0$. Since the leader is already on its desired trajectory, we have the error states $\delta_{p_1} := p_1 - p_1^* = 0$ and $\delta_{v_1} := v_1 - v_1^* = 0$.

2) The first follower and the $n - 2$ followers

We define error states for each follower as $\delta_{p_i} := p_i - p_i^*$ and $\delta_{v_i} := v_i - v_i^*$. Stacking all the position and velocity errors we have $\delta_p = [\delta_{p_2}^T, \dots, \delta_{p_n}^T]^T$ and $\delta_v = [\delta_{v_2}^T, \dots, \delta_{v_n}^T]^T$. From (3) and the equations for \dot{g}_{12} and $\dot{\bar{g}}_{12}$, the error dynamics for the first follower is as follows

$$\begin{aligned} \dot{\delta}_{p_2} &= \delta_{v_2} \\ \dot{\delta}_{v_2} &= -k_p P_{g_{21}} g_{21}^* - k_p P_{\bar{g}_{21}} \bar{g}_{21}^* - k_v \left[\frac{P_{g_{21}}}{\|e_{21}\|} + \frac{P_{\bar{g}_{21}}}{\|\bar{e}_{21}\|} \right] \delta_{v_2} \end{aligned}$$

The vectors g_{21} and \bar{g}_{21} in terms of δ_{p_2} are given by

$$d_{21} g_{21} = -\delta_{p_2} + e_{21}^*, \quad \bar{d}_{21} \bar{g}_{21} = -\delta_{p_2} + \bar{e}_{21}^*, \quad (4)$$

where $d_{21} = \|-\delta_{p_2} + e_{21}^*\|$ and $\bar{d}_{21} = \|-\delta_{p_2} + \bar{e}_{21}^*\|$. Thus $\dot{\delta}_{v_2}$ is a function of δ_{p_2} and δ_{v_2} . Similarly, from (2), the error dynamics for agent 3 is

$$\begin{aligned} \dot{\delta}_{p_3} &= \delta_{v_3} \\ \dot{\delta}_{v_3} &= -k_p P_{g_{31}} g_{31}^* - k_p P_{g_{32}} g_{32}^* - k_v \frac{P_{g_{31}}}{\|e_{31}\|} \delta_{v_3} + \frac{P_{g_{32}}}{\|e_{32}\|} (\delta_{v_2} - \delta_{v_3}) \end{aligned}$$

Similarly, the bearing vectors g_{31} and g_{32} can be written as

$$d_{31} g_{31} = -\delta_{p_3} + e_{31}^*, \quad d_{32} g_{32} = \delta_{p_2} - \delta_{p_3} + e_{32}^* \quad (5)$$

where $d_{31} = \|-\delta_{p_3} + e_{31}^*\|$ and $d_{32} = \|\delta_{p_2} - \delta_{p_3} + e_{32}^*\|$, making $\dot{\delta}_{v_3}$ a function of δ_{p_2} , δ_{p_3} , δ_{v_2} and δ_{v_3} . As every agent, v_i , for $i > 3$ has 2 neighbors, their corresponding error dynamics assumes a similar form as that of agent v_3 . Thus, we write

$$\dot{\delta}_p = \begin{bmatrix} \delta_{v_2} \\ \delta_{v_3} \\ \vdots \\ \delta_{v_n} \end{bmatrix} \quad \dot{\delta}_v = \begin{bmatrix} f_2(\delta_{p_2}, \delta_{v_2}) \\ f_3(\delta_{p_2}, \delta_{p_3}, \delta_{v_2}, \delta_{v_3}) \\ \vdots \\ f_n(\delta_{p_k}, \delta_{p_l}, \delta_{p_n}, \delta_{v_k}, \delta_{v_l}, \delta_{v_n}) \end{bmatrix} \quad (6)$$

where agents v_k and v_l are the neighbors of v_n ($v_k, v_l \in \mathcal{N}_n$). Before we characterize the equilibrium points of the error dynamics in (6), we introduce two important definitions of the terms *path of least indices*, and *formation scale*.

Definition 2 (Path of least indices): A sum of a sequence of edge vectors starting from any agent, v_i , to the leader, v_1 , in a given target formation, of the form

$$E_{i1}^* = e_{ij}^* + e_{jk}^* + \dots + e_{oq}^* + e_{q1}^*,$$

where $v_j \in \mathcal{N}_i, v_k \in \mathcal{N}_j, \dots, v_1 \in \mathcal{N}_q$, such that j, k, \dots, q are the least indices in $\mathcal{N}_i, \mathcal{N}_j, \dots, \mathcal{N}_o$, respectively is defined as the path of least indices for vertex v_i .

Definition 3 (Formation Scale [14]): For an LFF framework, $\mathcal{G}(p)$, formation scale is defined as the average of all the inter-agent distances defined on the edge set, \mathcal{E} , and is given by, $s(\mathcal{G}(p)) = \frac{1}{|\mathcal{E}|} \sum_{(v_i, v_j) \in \mathcal{E}} d_{ij}$.

Lemma 1: The relative bearing constraints g_{21}^* and \bar{g}_{21}^* fix the distance d_{21} between the leader and the first follower to some desired value d_{21}^* , thereby fixing the formation scale.

Proof: The two bearing vectors g_{21} and \bar{g}_{21} are related to each other by the constant radius vector as (see Fig. 2)

$$\bar{d}_{21} \bar{g}_{21} - d_{21} g_{21} = \hat{r}, \quad (7)$$

where $\bar{d}_{21} = \|\bar{e}_{21}\|, d_{21} = \|e_{21}\|$. The positions p_1, \bar{p}_1 and p_2 form a right angled triangle (say $p_1 p_2 \bar{p}_1$) with a fixed base which is the radius vector \hat{r} . Once the relative bearing constraints g_{21}^* and \bar{g}_{21}^* are specified, the angle between the two sides $p_1 p_2$ and $p_2 \bar{p}_1$ of the triangle gets specified. Hence, for the angle specified by the desired bearing constraints and the fixed base of the right angled triangle, there exist unique scalars \bar{d}_{21}^* and d_{21}^* such that (7) is satisfied, i.e., $\bar{d}_{21}^* \bar{g}_{21}^* - d_{21}^* g_{21}^* = \hat{r}$. Finally, we refer the reader to [14, Lemma 3] for the proof that d_{21}^* determines the scale of the formation. ■ Note that d_{21} gets fixed at d_{21}^* even when the conditions $g_{21} = -g_{21}^*$ and $\bar{g}_{21} = -\bar{g}_{21}^*$ hold.

Theorem 1: Under Assumptions 1-4, the error dynamics for the $n-1$ agent system in (6) has two equilibrium points: (a) $\delta_p = 0$ (when $g_{ij} = g_{ij}^* \forall (\mathbf{v}_i, \mathbf{v}_j) \in \mathcal{E}$), $\delta_v = 0$ (b) $\delta_p = 2E^* = 2[E_2^{*T} \ E_3^{*T} \ \dots \ E_n^{*T}]^T$ where $E_i^* = E_{i1}^*$ (when $g_{ij} = -g_{ij}^* \forall (\mathbf{v}_i, \mathbf{v}_j) \in \mathcal{E}$), $\delta_v = 0$.

Proof: From (6), $\dot{\delta}_p = 0$ gives $\delta_v = 0$, substituting this in $\dot{\delta}_v = 0$, we have

$$-k_p \begin{bmatrix} P_{g_{21}} g_{21}^* + P_{\bar{g}_{21}} \bar{g}_{21}^* \\ P_{g_{31}} g_{31}^* + P_{g_{32}} g_{32}^* \\ \vdots \\ P_{g_{nk}} g_{nk}^* + P_{g_{nl}} g_{nl}^* \end{bmatrix} = 0 \quad (8)$$

We now consider the first equation in (8), which corresponds to the first follower: $P_{g_{21}} g_{21}^* + P_{\bar{g}_{21}} \bar{g}_{21}^* = 0$. Premultiplying this with g_{21}^T we obtain $g_{21}^T P_{g_{21}} g_{21}^* + g_{21}^T P_{\bar{g}_{21}} \bar{g}_{21}^* = 0 \implies g_{21}^T P_{\bar{g}_{21}} \bar{g}_{21}^* = 0$. This is possible if $\bar{g}_{21} = \pm g_{21}$, which would imply that the leader is simple point in space, contradicting Assumption 3. Hence the only possibility is when $\bar{g}_{21} = \pm \bar{g}_{21}^*$. Substituting this in $P_{g_{21}} g_{21}^* + P_{\bar{g}_{21}} \bar{g}_{21}^* = 0$, it follows that $g_{21} = \pm g_{21}^*$. Note that the combinations $g_{21} = g_{21}^*$, $\bar{g}_{21} = -\bar{g}_{21}^*$ and $g_{21} = -g_{21}^*$, $\bar{g}_{21} = \bar{g}_{21}^*$ are physically unrealizable in \mathbb{R}^2 . When $g_{21} = g_{21}^*$ and $\bar{g}_{21} = \bar{g}_{21}^*$, from Lemma 1, we have $d_{21} = d_{21}^*$. This, along with equations in (4), leads to $\delta_{p_2} = 0$. Taking $g_{21} = -g_{21}^*$ and $\bar{g}_{21} = -\bar{g}_{21}^*$ in (4), we see that $\delta_{p_2} = 2e_{21}^*$, observe that the path of least indices for the first follower is $E_{21}^* = e_{21}^*$. We next consider the equation corresponding to agent \mathbf{v}_3 in (8): $P_{g_{31}} g_{31}^* + P_{g_{32}} g_{32}^* = 0$. Premultiplying this with g_{31}^T we obtain $g_{31}^T P_{g_{31}} g_{31}^* + g_{31}^T P_{g_{32}} g_{32}^* = 0 \implies g_{31}^T P_{g_{32}} g_{32}^* = 0$. This holds when $g_{31} = \pm g_{32}$, which suggests that agent \mathbf{v}_3 is collinear with the first follower and the leader. This along with $g_{21} = \pm g_{21}^*$ we have $P_{g_{31}} = P_{g_{32}} = P_{g_{21}^*}$. Substituting this in second equation of (8), we get $P_{g_{21}^*} (g_{31}^* + g_{32}^*) = 0 \implies g_{31}^* + g_{32}^* = \kappa g_{21}^*$, where κ is a scalar. Since agent \mathbf{v}_3 in the desired target formation is coplanar with \mathbf{v}_1 and \mathbf{v}_2 there exist nonzero positive constants d_{31}^* and d_{32}^* such that $d_{21}^* g_{21}^* + d_{32}^* g_{32}^* - d_{31}^* g_{31}^* = 0$, can be further simplified as $\frac{d_{21}^*}{\kappa} (g_{31}^* + g_{32}^*) + d_{32}^* g_{32}^* - d_{31}^* g_{31}^* = 0 \implies (d_{21}^* - \kappa d_{31}^*) g_{31}^* + (d_{21}^* + \kappa d_{32}^*) g_{32}^* = 0$. This shows that g_{31}^* and g_{32}^* are parallel and implies that agent \mathbf{v}_3 is collinear with the leader and agent \mathbf{v}_2 in the target formation, which contradicts Assumption 2. Thus, $g_{31} = \pm g_{32}$ does not hold and the only other possibility is $g_{31} = \pm g_{31}^*$. Substituting in $P_{g_{31}} g_{31}^* + P_{g_{32}} g_{32}^* = 0$, it immediately follows that $g_{32} = \pm g_{32}^*$. Considering $\delta_{p_2} = 0$ with $g_{31} = g_{31}^*$, $g_{32} = g_{32}^*$, from Lemma 1 we have $d_{31} = d_{31}^*$, $d_{32} = d_{32}^*$. Combining this with equations in (5), we have $d_{31}^* g_{31}^* = -\delta_{p_3} + e_{31}^*$, and $d_{32}^* g_{32}^* = -\delta_{p_3} + e_{32}^*$, which implies $\delta_{p_3} = 0$. Note that when $\delta_{p_2} = 0$ the combinations $g_{31} = g_{31}^*$, $g_{32} = -g_{32}^*$ or $g_{31} = -g_{31}^*$, $g_{32} = g_{32}^*$ or $g_{31} = -g_{31}^*$, $g_{32} = -g_{32}^*$ are physically unrealizable in \mathbb{R}^2 . Similarly when $\delta_{p_2} = 2e_{21}^*$, the only realizable conditions are $g_{31} = -g_{31}^*$ and $g_{32} = -g_{32}^*$. Hence, equations in (5) lead to $-d_{31}^* g_{31}^* = -\delta_{p_3} + e_{31}^*$, $-d_{32}^* g_{32}^* = 2e_{21}^* - \delta_{p_3} + e_{32}^*$. For $\delta_{p_3} = 2e_{31}^*$, both the conditions in (5) hold. Observe that the path of least indices for agent \mathbf{v}_3 is $E_{31}^* = e_{31}^*$. For every agent \mathbf{v}_i , $i \geq 4$, similar arguments as agent \mathbf{v}_3 show that when $\delta_{p_j} = 0, \delta_{p_k} = 0$ with $g_{ij} = g_{ij}^*, g_{ik} = g_{ik}^*$

we have $\delta_{p_i} = 0$, and when $\delta_{p_j} = 2E_{j1}^*, \delta_{p_k} = 2E_{k1}^*$ with $g_{ij} = -g_{ij}^*, g_{ik} = -g_{ik}^*$ we have $\delta_{p_i} = 2E_{i1}^*$ ($\mathbf{v}_j, \mathbf{v}_k \in \mathcal{N}_i$). ■ When $\delta_p = 2E^*$, geometrically the formation shape is a reflection of the desired formation shape about the leader as illustrated in Fig 3. We now linearize the error dynamics

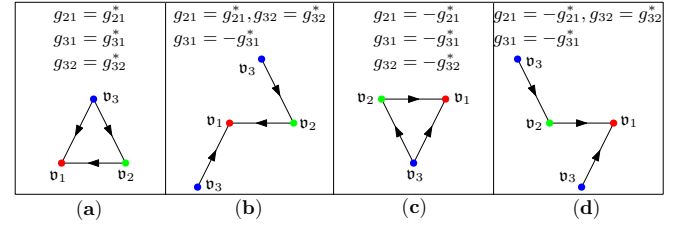


Fig. 3. Illustration of unrealizable bearing constraints in \mathbb{R}^2

in (6) around the two equilibrium points to investigate their local stability. Expressing the error dynamics as $[\dot{\delta}_p^T \ \dot{\delta}_v^T]^T = [\delta_v^T \ f^T(\delta_p, \delta_v)]^T$, the Jacobian can be expressed as

$$A := \begin{bmatrix} \partial(\delta_v)/\partial\delta_p & \partial(\delta_v)/\partial\delta_v \\ \partial(f(\delta_p, \delta_v))/\partial\delta_p & \partial(f(\delta_p, \delta_v))/\partial\delta_v \end{bmatrix} = \begin{bmatrix} \mathbf{0}_{2(n-1)} & \mathbf{I}_{2(n-1)} \\ A_{21} & A_{22} \end{bmatrix}$$

The elements of A for the first follower, \mathbf{v}_2 , are:

$$\frac{\partial f_2}{\partial \delta_{p_2}} = -k_p \left(G_{21} \frac{P_{g_{21}}}{\|e_{21}\|} + \bar{G}_{21} \frac{P_{\bar{g}_{21}}}{\|\bar{e}_{21}\|} \right); \quad \frac{\partial f_2}{\partial \delta_{v_2}} = -k_v \left(\frac{P_{g_{21}}}{\|e_{21}\|} + \frac{P_{\bar{g}_{21}}}{\|\bar{e}_{21}\|} \right)$$

$G_{21} = g_{21}^T g_{21}^* I_2 + g_{21} g_{21}^{*T}$, and $\bar{G}_{21} = \bar{g}_{21}^T \bar{g}_{21}^* I_2 + \bar{g}_{21} \bar{g}_{21}^{*T}$. The elements of A for followers $\mathbf{v}_i, i \in \{3, \dots, n\}$ are:

1. When $\mathbf{v}_j \notin \mathcal{N}_i$, $\frac{\partial f_i}{\partial \delta_{p_j}} = \frac{\partial f_i}{\partial \delta_{v_j}} = \mathbf{0}_2$.
2. When $\mathbf{v}_j \in \mathcal{N}_i$ and $i \neq j$

$$\begin{aligned} \frac{\partial f_i}{\partial \delta_{p_j}} &= k_p G_{ij} \frac{P_{g_{ij}}}{\|e_{ij}\|} + k_v \frac{\partial}{\partial \delta_{p_j}} \left[\frac{P_{g_{ij}}}{\|e_{ij}\|} \right] (\delta_{v_j} - \delta_{v_i}) \quad (9) \\ \frac{\partial f_i}{\partial \delta_{v_j}} &= k_v \frac{P_{g_{ij}}}{\|e_{ij}\|}, \end{aligned}$$

3. When $\mathbf{v}_i \in \mathcal{V} \setminus \{1, 2\}$ and $\mathbf{v}_j, \mathbf{v}_k \in \mathcal{N}_i$

$$\begin{aligned} \frac{\partial f_i}{\partial \delta_{p_i}} &= -k_p \left[G_{ij} \frac{P_{g_{ij}}}{\|e_{ij}\|} + G_{ik} \frac{P_{g_{ik}}}{\|e_{ik}\|} \right] + k_v \frac{\partial}{\partial \delta_{p_i}} \left[\frac{P_{g_{ij}}}{\|e_{ij}\|} \right] (\delta_{v_j} - \delta_{v_i}) \\ &\quad + k_v \frac{\partial}{\partial \delta_{p_i}} \left[\frac{P_{g_{ik}}}{\|e_{ik}\|} \right] (\delta_{v_k} - \delta_{v_i}) \quad (10) \end{aligned}$$

$$\frac{\partial f_i}{\partial \delta_{v_i}} = -k_v \left[\frac{P_{g_{ij}}}{\|e_{ij}\|} + \frac{P_{g_{ik}}}{\|e_{ik}\|} \right]$$

where $G_{ij} = g_{ij}^T g_{ij}^* I_2 + g_{ij} g_{ij}^{*T}$.

Theorem 2: The origin of the error dynamics $\delta_p = 0, \delta_v = 0$, for the $n-1$ agent system is locally asymptotically stable.

Proof: From the calculations above, the Jacobian evaluated at $\delta_p = 0, \delta_v = 0$ is given by $A|_{(0,0)} = \begin{bmatrix} \mathbf{0} & \mathbf{I} \\ -k_p L & -k_v L \end{bmatrix}$. The matrix $L \in \mathbb{R}^{2(n-1) \times 2(n-1)}$ has the following 2×2 block entries:

$$\begin{cases} [L]_{ij} = \mathbf{0}_2, & i \neq 1, i \neq j, (\mathbf{v}_i, \mathbf{v}_j) \notin \mathcal{E}, \\ [L]_{ij} = -\frac{P_{g_{ij}^*}}{\|e_{ij}^*\|}, & i \neq 1, i \neq j, (\mathbf{v}_i, \mathbf{v}_j) \in \mathcal{E} \\ [L]_{22} = \frac{P_{g_{21}^*}}{\|e_{21}^*\|} + \frac{P_{\bar{g}_{21}^*}}{\|\bar{e}_{21}^*\|} \\ [L]_{ii} = \frac{P_{g_{ij}^*}}{\|e_{ij}^*\|} + \frac{P_{g_{ik}^*}}{\|e_{ik}^*\|} & i \in \{3, 4, \dots, n\}, \text{ and } \mathbf{v}_j, \mathbf{v}_k \in \mathcal{N}_i. \end{cases}$$

Here the index $i \in \{2, \dots, n\}$, hence the first block matrix entry of L is denoted by $[L]_{22}$ (unconventionally). The matrix L may be obtained from a sub-matrix (\tilde{L}_B) of the modified bearing Laplacian \bar{L}_B in [16]. We get \tilde{L}_B by deleting the row blocks $[\bar{L}_B]_{1j}$ and column blocks $[\bar{L}_B]_{j1}$ $j = 1, \dots, n$ of \bar{L}_B corresponding to the leader. Thus,

$$\bar{L}_B = \begin{bmatrix} \mathbf{0}_d & \mathbf{0}_d & \mathbf{0}_d & \cdots & \mathbf{0}_d \\ -\frac{P_{g_{21}^*}}{\|e_{21}^*\|} & \frac{P_{g_{21}^*}}{\|e_{21}^*\|} & \mathbf{0}_d & \cdots & \mathbf{0}_d \\ * & * & \Sigma_3 & \cdots & * \\ \vdots & \vdots & \vdots & \ddots & \vdots \\ * & * & * & \cdots & \Sigma_n \end{bmatrix}, \tilde{L}_B = \begin{bmatrix} \frac{P_{g_{21}^*}}{\|e_{21}^*\|} & \mathbf{0}_d & \cdots & \mathbf{0}_d \\ * & \Sigma_3 & \cdots & * \\ \vdots & \vdots & \ddots & \vdots \\ * & * & \cdots & \Sigma_n \end{bmatrix},$$

where $\Sigma_i = \left[\frac{P_{g_{ij}^*}}{\|e_{ij}^*\|} + \frac{P_{g_{ik}^*}}{\|e_{ik}^*\|} \right]$, $\mathbf{v}_j, \mathbf{v}_k \in \mathcal{N}_i$. Adding $\frac{P_{g_{21}^*}}{\|e_{21}^*\|}$ to the first block element of \tilde{L}_B gives us the matrix L . Essentially, L differs from \tilde{L}_B at just one block, $[L]_{22}$. In the proof of [16, Lemma 5], it follows that either \bar{L}_B is in a block lower triangular structure or it can be transformed into a block lower triangular structure through appropriate permutation matrices. Hence \tilde{L}_B , and thus L , can be transformed to a block lower triangular structure. Since L is block lower triangular, its eigenvalues are the same as the union of the eigenvalues of the diagonal blocks therein. Now, $[L]_{22}$ is the sum of two symmetric positive semi-definite matrices whose null spaces intersect at $\{0\}$. Therefore the first two eigenvalues of L , corresponding to those of $[L]_{22}$, are positive real. The remaining $2(n-2)$ eigenvalues of L are same as those of \tilde{L}_B , which, in turn, are same as the last $2(n-2)$ eigenvalues of \bar{L}_B which have been shown to be positive real [16, Lemma 5]. Hence, all the eigenvalues of L are positive real, implying that the eigenvalues of $-L$ will be negative real. Now the eigenvalues of A are the roots of its characteristic polynomial given by $\det(\lambda I_{4(n-1)} - A)$ and can be written as $\lambda_{i\pm} = \frac{1}{2} [k_v \mu_i \pm \sqrt{k_v^2 \mu_i^2 + 4k_p \mu_i}]$, where μ_i are eigenvalues of $-L$ (see [21]). The term under the radical, $k_v^2 \mu_i^2 + 4k_p \mu_i$, evaluates to either a positive or negative real number since μ_i, k_p, k_v are real. When it evaluates to a negative real number, $\sqrt{k_v^2 \mu_i^2 + 4k_p \mu_i}$ is purely imaginary, leading to a complex conjugate pair of eigenvalues with negative real parts for the Jacobian A . When it evaluates to a positive real number, the root $\lambda_{i-} = \frac{1}{2} (k_v \mu_i - \sqrt{k_v^2 \mu_i^2 + 4k_p \mu_i})$ will be a negative real number. Now, consider the root λ_{i+} given by $\lambda_{i+} = \frac{1}{2} (k_v \mu_i + \sqrt{k_v^2 \mu_i^2 + 4k_p \mu_i}) = \frac{|k_v \mu_i|}{2} (-1 + \sqrt{1 + (4k_p/k_v^2 \mu_i)})$. We have $\sqrt{1 + (4k_p/k_v^2 \mu_i)} < 1$ since $\mu_i < 0$ and $k_p, k_v > 0$, which implies that λ_{i+} will also be a negative real root of the Jacobian A . It then follows that the Jacobian A is Hurwitz and hence, from *Theorem 4.7* of [22], we conclude that the system is locally asymptotically stable about $\delta_p = 0, \delta_v = 0$. ■

Theorem 3: The equilibrium $\delta_p = 2E^*, \delta_v = 0$ of the error dynamics (6) for the $n-1$ followers is unstable.

Proof: At $\delta_{p_i} = 2E_{i1}^*$ we have $G_{ij} = (P_{g_{ij}^*}/\|e_{ij}^*\|)$ in (9) and (10). The Jacobian takes the form $A|_{(2E^*, 0)} = \begin{bmatrix} \mathbf{0} & \mathbf{I} \\ k_p L & -k_v L \end{bmatrix}$. The eigenvalues of the Jacobian, $\lambda_{i\pm}$, and that of $-L$, say μ_i , are related as $\lambda_{i\pm} = \frac{1}{2} (k_v \mu_i \pm \sqrt{k_v^2 \mu_i^2 - 4k_p \mu_i})$. The term $k_v^2 \mu_i^2 - 4k_p \mu_i$, will be pos-

itive since $\mu_i < 0$. Hence the root $\lambda_{i-} = \frac{1}{2} (k_v \mu_i - \sqrt{k_v^2 \mu_i^2 - 4k_p \mu_i})$ will be a negative real number. Now, consider the root λ_{i+} given as $\lambda_{i+} = \frac{1}{2} (k_v \mu_i + \sqrt{k_v^2 \mu_i^2 - 4k_p \mu_i}) = \frac{|k_v \mu_i|}{2} (-1 + \sqrt{1 - (4k_p/k_v^2 \mu_i)})$, as $\mu_i < 0$ and $k_p, k_v > 0$ we have $(1 - (4k_p/k_v^2 \mu_i)) > 1$. Therefore, $(-1 + \sqrt{1 - (4k_p/k_v^2 \mu_i)}) > 0$ which implies λ_{i+} is positive real. Hence, for every negative eigenvalue, μ_i of $-L$, there is one positive root λ_{i+} and one negative root λ_{i-} for the Jacobian and thus has $2(n-1)$ positive real roots. From [22, Theorem 4.7], the equilibrium $\delta_p = 2E^*, \delta_v = 0$ is unstable. ■

IV. ILLUSTRATIVE EXAMPLES

A system of 4 agents is considered, with the desired formation shape being a square and the edge set consists of $|\mathcal{E}| = 5$ directed edges. The radius of the leader is taken as $r = 3$ units and the design parameters are chosen as $k_p = 1$ and $k_v = 20$. The desired bearing constraints are given by $g_{21}^* = [-1 \ 0]^T$, $\bar{g}_{21}^* = [-\frac{\sqrt{216}}{15} \ \frac{3}{15}]^T$, $g_{32}^* = [0 \ -1]^T$, $g_{31}^* = \frac{1}{\sqrt{2}}[-1 \ -1]^T$, $g_{43}^* = [1 \ 0]^T$ and $g_{41}^* = [0 \ -1]^T$. In every figure, green and blue circles (○) represent initial positions for first follower and other followers respectively, while the leader is a red triangle (▷). Solid green and blue circles (●) represent final positions of the first follower and the other followers respectively and solid red triangle (▶) represents the leader. The dashed and solid black lines show the initial and final formation shape.

For the simulations shown Fig 4, the control law described by equation (2) in [16] is applied to all the agents. In Fig 4(a) the distance d_{21} continues to decrease leading to an undesirable scenario of consensus among agents. From Fig 4(b) we see that the bearing error converges to zero, indicating that formation shape was achieved and the scale decreased continuously. Fig 4(c) represents the case when the distance d_{21} continued to increase with time as shown in Fig 4(d). Here, yet again, the desired formation shape was achieved but the inter-agent distances increased with time leading to a formation whose scale increased continuously. For the simulations shown in Fig 5(a) and Fig 5(c), the control law in equations (3) and (2) are applied to the first follower and the remaining three agents respectively. The initial conditions for Fig 5(a) and Fig 5(c) are identical to that of simulations in Fig 4(a) and Fig 4(c), respectively. Fig 5(b) and Fig 5(d) show the distance d_{21} settling to the desired value.

V. CONCLUSIONS

We studied a bearing-only formation control law for double integrator agents with LFF structure formations. We show that formation scale can be controlled with bearing and bearing rates if the leaders physical dimensions are considered to be non-trivial. We also showed that the multi-agent system under the proposed control law has two equilibria of which the desired one is locally stable while the undesired equilibrium is unstable. From the numerous simulations carried out we conjecture that the region of attraction around the desired formation shape is significantly large. Hence the

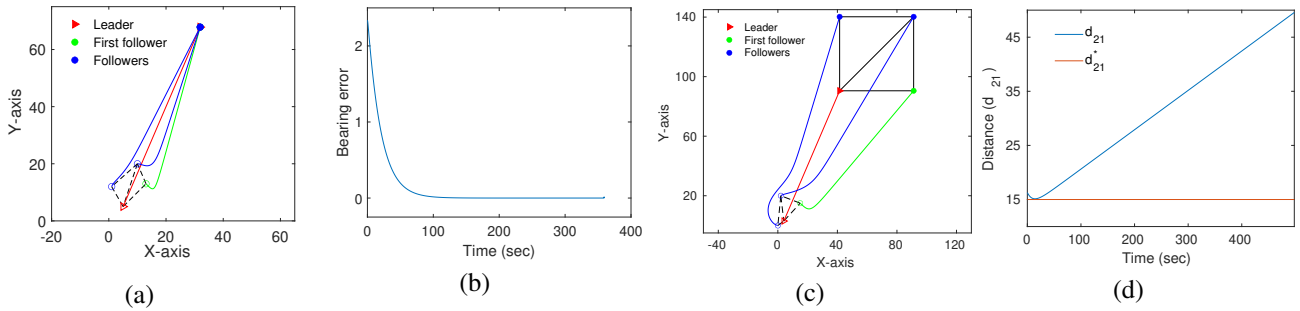


Fig. 4. (a): Undesired consensus resulting from the absence of the bearing constraint \bar{g}_{21} , (b): Bearing error ($\sum_{(v_i, v_j) \in \mathcal{E}} \|g_{ij} - g_{ij}^*\|$) converges to zero and is undefined at the point of consensus, (c): Increasing inter-agent distances in the absence of \bar{g}_{21} , (d): Distance d_{21} increases with time

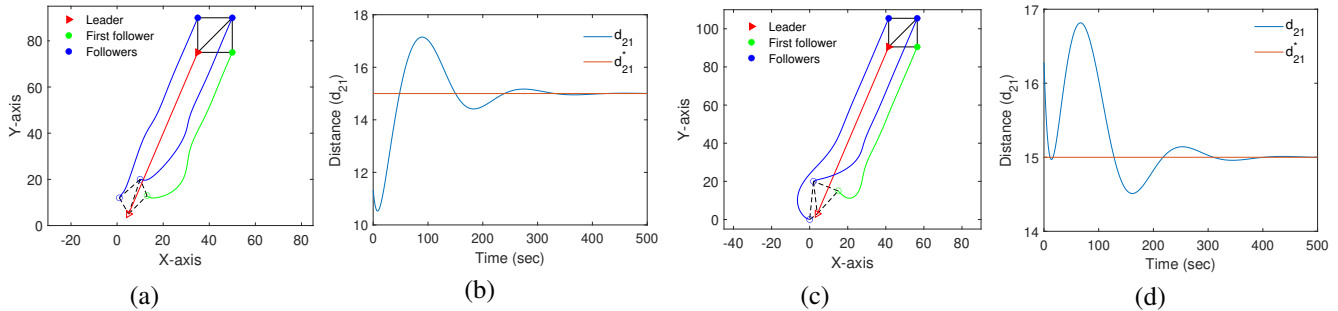


Fig. 5. (a) and (c): Formation when bearing constraint \bar{g}_{21} is considered, (b) and (d): distance d_{21} settling at the desired value $d_{21}^* = 15$

immediate future goal is to conduct deeper investigation of the global behaviour of the agents and to extend the results presented here to three dimensional Euclidean space.

REFERENCES

- [1] M. Mesbahi and M. Egerstedt, *Graph theoretic methods in multiagent networks*. Princeton University Press, 2010.
- [2] R. Olfati-Saber and R. M. Murray, "Distributed cooperative control of multiple vehicle formations using structural potential functions," *IFAC Proceedings Volumes*, vol. 35, no. 1, pp. 495–500, 2002.
- [3] K.-K. Oh, M.-C. Park, and H.-S. Ahn, "A survey of multi-agent formation control," *Automatica*, vol. 53, pp. 424–440, 2015.
- [4] B. D. Anderson, C. Yu, B. Fidan, and J. M. Hendrickx, "Rigid graph control architectures for autonomous formations," *IEEE Control Systems Magazine*, vol. 28, no. 6, pp. 48–63, 2008.
- [5] J. M. Hendrickx, B. D. Anderson, J.-C. Delvenne, and V. D. Blondel, "Directed graphs for the analysis of rigidity and persistence in autonomous agent systems," *International Journal of Robust and Nonlinear Control: IFAC-Affiliated Journal*, vol. 17, no. 10-11, pp. 960–981, 2007.
- [6] Z. Sun, B. D. Anderson, M. Deghat, and H.-S. Ahn, "Rigid formation control of double-integrator systems," *International Journal of Control*, vol. 90, no. 7, pp. 1403–1419, 2017.
- [7] R. Tron, J. Thomas, G. Loianno, K. Daniilidis, and V. Kumar, "A distributed optimization framework for localization and formation control: Applications to vision-based measurements," *IEEE Control Systems Magazine*, vol. 36, no. 4, pp. 22–44, 2016.
- [8] S. Zhao and D. Zelazo, "Bearing rigidity theory and its applications for control and estimation of network systems: Life beyond distance rigidity," *IEEE Control Systems Magazine*, vol. 39, no. 2, 2019.
- [9] S. Zhao, Z. Li, and Z. Ding, "Bearing-only formation tracking control of multiagent systems," *IEEE Transactions on Automatic Control*, vol. 64, no. 11, pp. 4541–4554, 2019.
- [10] S. Zhao and D. Zelazo, "Translational and scaling formation maneuver control via a bearing-based approach," *IEEE Transactions on Control of Network Systems*, vol. 4, pp. 429–438, 2015.
- [11] R. Tron, J. Thomas, G. Loianno, K. Daniilidis, and V. Kumar, "Bearing-only formation control with auxiliary distance measurements, leaders, and collision avoidance," in *2016 IEEE 55th Conference on Decision and Control (CDC)*. IEEE, 2016, pp. 1806–1813.
- [12] S. Zhao and D. Zelazo, "Bearing-based formation stabilization with directed interaction topologies," in *2015 54th IEEE Conference on Decision and Control (CDC)*. Japan: IEEE, 2015, pp. 6115–6120.
- [13] M. Trinh, D. Mukherjee, D. Zelazo, and H. Ahn, "Formations on directed cycles with bearing-only measurements," *International Journal of Robust and Nonlinear Control*, vol. 28, pp. 1074–1096, 2018.
- [14] M. H. Trinh, S. Zhao, Z. Sun, D. Zelazo, B. D. Anderson, and H.-S. Ahn, "Bearing-based formation control of a group of agents with leader-first follower structure," *IEEE Transactions on Automatic Control*, vol. 64, no. 2, pp. 598–613, 2018.
- [15] Z. Tang, R. Cunha, T. Hamel, and C. Silvestre, "Formation control of a leader–follower structure in three dimensional space using bearing measurements," *Automatica*, vol. 128, p. 109567, 2021.
- [16] S. T. Rayabagi, D. Pal, and D. Mukherjee, "Bearing-only formation control for double integrators in a plane," *IFAC-PapersOnLine*, vol. 55, no. 22, pp. 275–280, 2022.
- [17] N. P. K. Chan, B. Jayawardhana, and H. G. de Marina, "Angle-constrained formation control for circular mobile robots," *IEEE Control Systems Letters*, vol. 5, no. 1, pp. 109–114, 2021.
- [18] L. Chen and Z. Sun, "Gradient-based bearing-only formation control: An elevation angle approach," *Automatica*, vol. 141, p. 110310, 2022.
- [19] C. Garanayak and D. Mukherjee, "Bearing-only formation control using sign-elevation angle rigidity for avoiding formation ambiguities," in *2023 American Control Conference (ACC)*, 2023, pp. 2684–2689.
- [20] T. Eren, "Formation shape control based on bearing rigidity," *International Journal of Control*, vol. 85, no. 9, pp. 1361–1379, 2012.
- [21] W. Ren and E. Atkins, "Second-order consensus protocols in multiple vehicle systems with local interactions," in *AIAA guidance, navigation, and control conference and exhibit*, 2005, p. 6238.
- [22] H. K. Khalil, *Nonlinear Systems*, 3rd ed. Prentice Hall, 2002.